File Revision Date:
October, 2023

Data set Description:
PI: G. Ancellet
Instrument: UV DIAL lidar
Site: Observatoire de Haute Provence
Measurement Quantities: Vertical profile of tropospheric ozone

Contact Information:
Name: G. Ancellet
Address: Latmos UMR8190, Sorbonne Université, Boite 102
                            4 Place Jussieu 75252 Paris Cedex 05 France
Phone: 33 1 44 27 47 62
E. Mail: gerard.ancellet@latmos.ipsl.fr

References Articles:
G. Ancellet, A. Papayannis, J. Pelon, and G. Mégie, 1989: DIAL Tropospheric Ozone Measurement Using a Nd:YAG Laser and the Raman Shifting Technique. J. Atmos. Oceanic Technol., 6, 832¿839, https://doi.org/10.1175/1520-0426(1989)006<0832:DTOMUA>2.0.CO;2

G.Ancellet and M.Beekmann. Evidence for changes in the ozone concentration in the free troposphere over Southern Europe from 1976--1995. Atmos. Environ., 31(17):2835--2851, 1997.

M.Beekmann, G.Ancellet, D.Martin, C.Abonnel, G.Duverneuil, F.Eideliman, P.Bessemoulin, N.Fritz, and E.Gizard. Intercomparison of tropospheric ozone profiles obtained by electrochemical sondes, a ground-based lidar and an airborne UV-photometer. Atmos. Environ., 29(9):1027--1042, 1995.

G.Ancellet and F.Ravetta. A compact airborne lidar for tropospheric ozone (alto): description and field measurements. Appl. Opt., 37:5509--5521, 1998.

A. Gaudel, G. Ancellet, S. Godin-Beekmann, Analysis of 20 years of tropospheric ozone vertical profiles by lidar and ECC at Observatoire de Haute Provence (OHP) at 44°N, 6.7°E, Atmospheric Environment, Volume 113, 2015, Pages 78-89, https://doi.org/10.1016/j.atmosenv.2015.04.028.

Wing R., Steinbrecht W., Godin-Beekmann S., Mcgee T. J., Sullivan J. T., Sumnicht G., Ancellet G., Hauchecorne A., Khaykin S., Keckhut P. *Atmospheric Measurement Techniques*, 2020, 13 (10), pp.5621-5642. ⟨10.5194/amt-13-5621-2020⟩

Ancellet G., Godin-Beekmann S., Smit H., Stauffer R., van Malderen R., Bodichon R., Pazmino A. Homogenization of the Observatoire de Haute Provence electrochemical concentration cell (ECC) ozonesonde data record: comparison with lidar and satellite observations, *Atmospheric Measurement Techniques*, 2022, 15 (10), pp.3105-3120. ⟨10.5194/amt-15-3105-2022⟩

Description of AMES data format

Header line description

Parameter 1: Lidar starting measurement time in Julian day

Parameter 2: number of altitude reported

Parameter 3 to 7: Lidar starting measurement time in year, month, day, hour (UT), minute

Parameter 8: Measurement time after starting date in hours

Parameter 9 to 11: OHP station position: latitude, longitude, altitude ASL in m

Parameter 12 to 15: Altitudes in km used for gluing analog and photocounting channels (Upper bound of analog channel and lower bound of photocounting channel) for the absorbed and reference wavelength

Parameter 16 and 19: Lower and upper altitudes in km with detection of clouds

Parameter 17 and 20: Lower and upper altitudes in km where another subset of lidar shots has been used for ozone retrieval inside the lidar measurement time in order to remove a first cloud altitude range

Parameter 18 and 21: Lower and upper altitudes in km where another subset of lidar shots has been used for ozone retrieval inside the lidar measurement time in order to remove a second cloud altitude range:

Parameter 22: Number of lidar shots integrated for the ozone retrieval

Parameter 23: laser frequency in Hz

Parameter 24: absorbed wavelength in nm

Parameter 25: reference wavelength in nm

Data column description

11 columns with altitude dependent parameters:

column 1: altitude ASL in m

column 2: ozone concentration in $mol.cm^{-3}$ (final retrieval)

column 3: relative error for ozone concentration retrieval in %

column 4: vertical resolution in m of numerical filter used for signal derivative calculation

column 5: as column 2 but without the overlap function correction (the comparison with col2 provides an upper limit of the error due to the geometrical overlap function correction)

column 6: Differential absorption cross-section in cm^2 used for the ozone retrieval

column 7: Model atmospheric density in $mol.cm^{-3}$ for the Rayleigh scattering correction and O_3 mixing ratio retrieval

column 8: Differential absorption due to Rayleigh scattering in cm^{-1}

column 9: Differential vertical log derivative of the Rayleigh backscatter profile in cm^{-1} (only relevant when aerosol correction is applied for the ozone retrieval)

column 10: overlap function at the absorbed wavelength

column 11: overlap function at the reference wavelength

Instrument Description:

A Nd-YAG laser is used in combination with a Raman cell filled up with Deuterium or Hydrogen to generate two wavelengths simultaneously transmitted to the atmosphere: 289 and 299 nm (before

March 1993) and 289-316 nm (since March 1993). A 80-cm telescope is used to collect the backscattered light and is coupled to a grating spectrometer for wavelength separation and background sky light filtering. The full geometrical overlap between the telscope field of view (1.0 mrd) and the laser beam is obtained at ranges above 5 km.

Output of 2 PhotoMultiplier Tubes (PMTs) are recorded by photocounting and analog detection. The combination of two different detection methods provides a dynamical range larger than 15 km for the lidar measurement in the free troposphere.

From 1990 to 2011, the data acquisition system was a homemade unit (12-bits, 10-MHz Analog Device ADC and 300 MHz counters operated with 250 ns time gates). Since 2012 the data acquisition system is a LICEL system with two TR-2080 transient recorder.

Although daytime measurements are possible with a range limited to 10 km, the lidar is usually operated at sunset to reduce the background noise at 316 nm. Lidar signal are usually averaged during 100 s (2000 laser shots) to produce level 0 observations. The level 0 observations are archived since 1990 in the LATMOS data base.
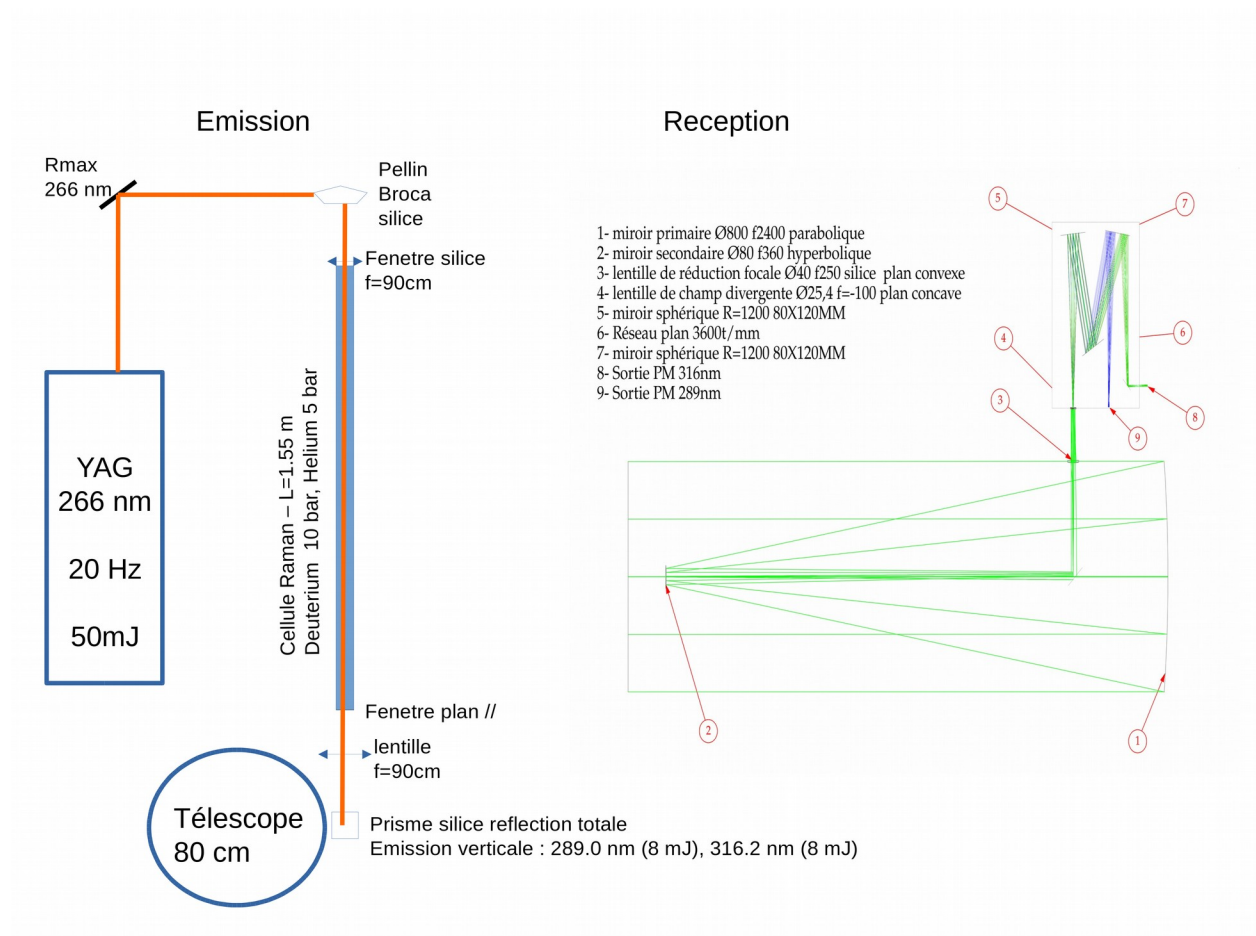
Fig. Layout of the optical configuration of the lidar

Data processing

The 100 s averages are further added to improve the signal to noise ratio. In practise, the integration time is of the order of 60 min. Range averaging of the range corrected signal is performed with a numerical low pass filter(fitting of a 2nd order polynomial) with a number of points increasing with range. The number of bins is calculated to obtain a range resolution of 150 m at 2 km ASL and 1000 m above 10 km ASL. The differential geometrical compression between the two wavelength is corrected using a model of the overlap function to retrieve ozone data down to a 1.8-km range (2.5 km ASL altitude). The divergence of the transmitted beams were determined experimentally for each wavelength. This misaligment angle at the reference wavelength is determined by fitting the 316-nm signal derivative to the molecular attenuation in the 1.5-3 km range and the misalignment difference between the two beams is checked by using comparisons with ECC ozonesonde profiles when they are made at night.

The background noise correction of the analog signal is optimized to obtain an overlap of the analog signal log derivative with the counting signal log derivative at ranges above 7 km when the photocounting is no more saturated. The background noise correction of the photocounting signal is optimized by fitting the lidar signal with a decreasing exponential function to account for detector overload at short ranges. The accuracy of the correction of the photcounting background noise is checked with the lower measurement range of the stratospheric ozone lidar when it is operated on the same night.

The ozone absorption cross sections used for the ozone calculation are taken after the work of Bass and Paur but using the Molina and Molina (1986) cross section temperature dependency at 289 and 316 nm. Correction of the molecular extinction (Rayleigh extinction) is based on ECMWF analysis interpolated at the OHP location and for the lidar time measurement.

Molina L. and M..Molina (1986) Absolute absorption cross sections of ozone in the 185 to 350 nm wavelength range, J.Geophys.Res., 91, D13, 14501-14508.

Error analysis

When no significant aerosol layers are present, the DIAL measurements are limited first by statistical errors related to the decreasing signal-to-noise ratio at far ranges and second by systematic errors arising from instrumental limitations, namely the correction of the geometrical overlap function at near range and the correction of background noise in the upper range. The error due to the correction of the overlap function can be obtained using the difference between the uncorrected and corrected ozone profiles (typically using half of this difference as the error upper bound). Only the statistical error are reported for the analog channels in the NDACC data files. For the photocounting channels, the background correction error is added to the statistical error due to signal detection. It is calculated assuming a 100% error on the background value so it becomes the major error at upper ranges above 10 km. Before 2012 residual noise at frequencies less than 50 kHz are been sometimes observed in the analog signals and are not always suppressed by averaging or filtering. It can be easily identified using

comparison plots of the signal derivative between analog and photocounting channels ou between 289 and 316 nm channels.

At near range below 4 km, the DIAL measurement remain subject to a bias related to differences between the geometrical telescope overlap function of each emitted laser beam and the telescope field of view. The shortest distance where measurement is possible even with a first order correction of the overlap fucntion is of the order of 1800 m to keep ozone error below 15 ppb at this altitude. The ozone profile without the correction of the overlap function is provided in the AMES file in order to calculate the upper bound of the error at ranges below 4 km (half of the difference between column 2 and column 5 is a good proxy of this upper bound).

The aerosol backscatter coefficient is calculated at 316 nm where ozone absorption is negligible, using a backward integration scheme described by (Browell et al., 1985). A 316-nm extinction to backscatter ratio of 50 is generally chosen corresponding to the average value for the different kind of continental aerosol encountered above the PBL at OHP. This information is used to verify whether significant aerosol layers are present in the measurement area, and correction are only made when a clear ozone first derivative distortion is observed on the zone vertical profile at the aerosol layer altitude. Angtrom coefficients for backscatter and extinction at 289 nm are taken from the range of data observed at 290 nm in the work of Eisele and Trickl (2005). Cloud layers are always identified and ozone data are removed from these area because no valuable corrections can be made in such conditions.

Browell, E., S.Ismail, and S.Shipley (1985) Ultraviolet DIAL measurements of ozone profiles in regions of spatially inhomogeneous aerosols, Appl.Opt., 24, 2827-2836.

Eisele H. and Trickl T. (2005) Improvements of the aerosol algorithm in ozone lidar data processing by use of evolutionary strategies, Applied Optics 44, 2638-2651,

Instrument history

1990-1993
Beginning of measurements in 1990 at OHP (limited number of profiles in 1990 and 1991)
    1) two Raman cells were used to generate the wavelengths 289, 299 nm
    2) the two-cell system was sensitive to the alignment below 5 km
    3) Old QUANTEL laser with unstable 4th harmonic generator

1993-2011
02/1993 Change of the laser (Continuum Surelite) and move to a single cell system as described above
11/1998 to 03/1999 Breakdown of the data acquisition system. Installation of a new waveform recorders.
05/2001 to 07/2002: Maintenance of laser and data acquisition system
08/2004 to 02/2005: Laser failure. Installation of a new SURELITE laser.

2012-2023
03/2012: New lidar optical design (shorter distance between laser optical table and telescope, optical
                     alignment becomes more stable)

Installation of the LICEL data acquisition TR2080 with analog and photocounting recording instead of the LATMOS home made system. The two PMTs are unchanged.

03/2013 to 12/2013: Several laser failure (4th harmonic generator). Installation of a Pellin Broca prism to decouple the laser and the Raman cell and to improve the 4th harmonic generator lifetime

02/12/2019: Installation of a new Lumibird laser (model QSMART 450, 20 Hz) with autophase matching module for the 266 nm output power.